Quasiclassical Trajectory Study of the $CH_3^+ + HD \rightarrow CH_2D^+ + H_2$ Reaction†

Kurt M. Christoffel,‡ Zhong Jin,|| Bastiaan J. Braams,§ and Joel M. Bowman*

Cherry L. Emerson Center for Scientific Computation and Department of Chemistry, 1521 Dickey Drive, Emory University, Atlanta, Georgia 30322

Received: December 19, 2006; In Final Form: February 1, 2007

A full dimensional *ab initio* potential energy surface for the CH_5^+ system based on coupled cluster electronic structure calculations and capable of describing the dissociation of methonium ion into methyl cation and molecular hydrogen (*J. Phys. Chem. A* **2006**, *110*, 1569) is used in quasiclassical trajectory calculations of the reaction $CH_3^+ + HD \rightarrow CH_2D^+ + H_2$ for low collision energies of relevance to astrochemistry. Cross sections for the exchange are obtained at several relative translational energies and a fit to the energy dependence of the cross sections is used to obtain the rate constant at temperatures between 10 and 50 K. The calculated rate constant at 10 K agrees well with the previously reported experimental value. Internal energy distributions of the products are presented and discussed in the context of zero-point energy "noncompliance".

1. Introduction

Deuterated molecular hydrogen, HD, is the primary reservoir of deuterium in the dark, dense clouds of the interstellar medium (ISM). At the temperature of the ISM (approximately 10 K) the reactions of significance are exothermic and without any substantial activation barrier, primarily ion−molecule reactions. Three molecular ions in dark, dense interstellar clouds, H_3^+, CH_3^+ and $C_2H_2^+$, are known to exchange deuterium with HD. The exothermicity of these exchange reactions arises from zero-point energy differences between reactants and products. Since the reverse reactions are endothermic (and hence very slow) these exchange processes can produce deuterated ion (e.g., CH_2D^+) : normal ion (e.g., CH_3^+) ratios that are orders of magnitude greater than the cosmic D:H ratio.[1,2] Rate constants (at approximately 10 K) for all three of these primary ion−molecule deuterium exchange reactions have been recently determined in a 22-pole ion trap apparatus.[3−5]

In recent years within the chemical community there has been renewed interest in the methonium ion, CH_5^+. Almost since its discovery[6] in 1952, the issue of whether or not CH_5^+, a species exhibiting an unusual 3-center−2-electron bond, has a "structure" has been a topic of speculation and (until recently largely theoretical) research.[7] This challenge motivated the pioneering density functional theory direct-dynamics studies of CH_5^+ by Marx and Parrinello[8−10] that supported a fluxional nature for CH_5^+. In 1999 the high-resolution infrared spectrum of CH_5^+ in the C−H stretching region (2770−3150 cm^{-1}) was first reported by Oka and co-workers[11] and even now largely defies assignment and interpretation due to the large-amplitude motions and hydrogen scrambling. Both a low-resolution laser-induced reaction (LIR) spectrum of CH_5^+ at 110 K (over the spectral range of 540−3250 cm^{-1})[12,13] and a high-resolution direct absorption spectrum of jet-cooled CH_5^+ (over the spectral range of 2825−3050 cm^{-1})[14] have been very recently reported and analyzed.

The development and refinement of a full dimensional potential energy surface (PES) in this lab has facilitated detailed dynamical studies of the CH_5^+ system.[15−18] The earlier versions of this surface[15−17] were limited to energies well below the $CH_3^+ + H_2$ dissociation threshold and were based on functional fitting of MP2 level electronic structure calculations. These surfaces were adequate for our earlier studies of bound CH_5^+ dynamics and for diffusion Monte Carlo characterization of the quantum ground state. The latest version of our CH_5^+ potential is based on higher quality CCSD(T)/aug-cc-pVTZ *ab initio* energies, has been extended to energies above the $CH_3^+ + H_2$ threshold and incorporates established potentials to describe long-range interactions.[18] We use this surface here and the quasiclassical trajectory (QCT) method to study the dynamics of the astrochemically significant $CH_3^+ + HD$ exchange reaction.

The remainder of this paper is organized as follows. In section 2, we provide a description of the potential energy surface, the implementation of the QCT method for determining reaction cross sections and the method used to determine the rate constant for the $CH_3^+ + HD$ exchange in the temperature range 10−50 K. Our results are presented and discussed in section 3. In section 4, we summarize the important results and conclusions of our work.

2. Computational Details

2.1. Potential Energy Surface. Initial work in our lab toward development of a full-dimensional global potential energy surface for the CH_5^+ system began late in 2002. The first reported version of the surface was based on Møller-Plesset perturbation theory (MP2)[19] level electronic structure calculations using the correlation consistent polarization triple-ζ (cc-pVTZ) basis set of Dunning.[20] These MP2/cc-pVTZ *ab initio* energies at 4096 unique geometries generated by direct dynamics trajectories at energies up to 8000 cm^{-1} above the CH_5^+ global minimum were fit to a functional form that ensures the full permutational symmetry of the system.[15] Subsequently additional MP2/cc-pVTZ results generated on grids in normal coordinates and a new functional fit were used to obtain a potential energy surface reliable up to 13 000 cm^{-1} above the CH_5^+ global minimum.[17]

The geometries used in these potentials were focused in the region of the CH_5^+ configuration space around the CH_5^+ global

† Part of the special issue "M. C. Lin Festschrift".

* Corresponding author. E-mail: jmbowma@emory.edu.

‡ Permanent address: Department of Chemistry, Augustana College, Rock Island, IL, 61201.

§ Present address: Department of Mathematics and Computer Science, Emory University, 400 Dowman Drive, Atlanta, GA, 30322.

|| Present address: Supercomputing Center of Computer Network Information Center, Chinese Academy of Sciences, Beijing, P. R. China.

10.1021/jp068722l CCC: $37.00 © 2007 American Chemical Society
Published on Web 03/13/2007

minimum and so do not describe dissociation of methonium ion into methyl cation and molecular hydrogen. Motivated by an interest in the astrochemically important processes of isotope exchange

$$CH_3^+ + HD \rightarrow CH_2D^+ + H_2 \quad (1)$$

and associative recombination,

$$CH_3^+ + H_2 \rightarrow CH_5^+ + h\nu \quad (2)$$

efforts were initiated to develop a potential energy surface suitable for dynamical studies of these processes. For this purpose higher quality CCSD(T) *ab initio* calculations using a larger aug-cc-pVTZ basis set were performed at 36 173 geometries (including geometries from the previous surfaces and thousands of additional configurations along the dissociation pathway). A "reaction coordinate" R can be defined as the distance between the carbon atom and the H_2 moiety. The CCSD(T)/aug-cc-pVTZ energy data-set was extended to R values as large as $15a_o$. These $R \leq 15a_o$ *ab initio* data were fit by a weighted least-squares method to a multinomial functional form containing 2302 terms in the 15 internuclear distances that ensures satisfaction of the permutational symmetry of the five hydrogens. The reader is referred to our earlier work, particularly refs 17 and 18, for details of the functional form, the fitting procedure, and properties of the PES.

A surface to be used in dynamical studies of reaction 1 at the very low relative translational energies of relevance in the ISM must also properly describe the long-range $CH_3^+-H_2$ interaction.[18] Rather than extending the *ab initio* calculations into the $R > 15a_o$ region, we followed the procedure adopted previously[21] for the H_5^+ potential energy surface which was to extend the fit using a simple switching function and the known long-range interaction of this singly charged ion-H_2 system. The switching is performed in the region $11a_o \leq R \leq 15a_o$ in which the potential is written as

$$V = V_{fit}[1 - S(R)] + V_{LR}S(R) \quad (3)$$

where the long-range potential is

$$V_{LR} = V_{ion-induced\ dipole} + V_{CH_3^+} + V_{H_2} + D_e \quad (4)$$

Here V_{fit} is the potential energy obtained from the fit to the *ab initio* data, $V_{ion-induced\ dipole}$ is a known analytical expression for the long-range interaction between CH_3^+ and H_2, $V_{CH_3^+}$ and V_{H_2} are the potentials of these fragments and D_e is the dissociation energy (of CH_5^+ into $CH_3^+ + H_2$). $S(R)$ is a polynomial switching function that over the finite interval $11a_o \leq R \leq 15a_o$ varies smoothly between 0 and 1.[22] $V_{CH_3^+}$ and V_{H_2} were obtained from the CH_5^+ fit at large separation where the fragments are weakly interacting. The long-range term $V_{ion-induced\ dipole}$ is given by the sum of U_4 charge-induced dipole (H_2) and U_3 charge-(H_2) quadrupole terms available in the literature.[23] Values of the polarizability and the quadrupole moment as needed were obtained by cubic spline interpolation of published data.[24,25] This potential henceforth referred to as the JBB (Jin−Braams−Bowman)[18] CH_5^+ potential is used in the dynamical studies of reaction 1 reported here. The most significant features of the JBB surface for the exchange reaction 1 are the absence of any barrier in the exit/entrance channel, a potential well depth for CH_5^+ of approximately 16 320 cm^{-1} (46.7 kcal/mol) relative to $CH_3^+ + H_2$, and a zero-point energy exothermicity for reaction 1 of 309 cm^{-1} (0.884 kcal/mol, 445 K).

TABLE 1: Reaction Cross Sections for $CH_3^+ + HD \rightarrow CH_2D^+ + H_2$ as a Function of Initial Relative Translational Energy[a]

E_{trans} (kcal/mol)	N_{max}	b_{max} (Å)	σ_1 (Å^2)	σ_2 (Å^2)	σ_{2-NOZP} (Å^2)
0.05	450 000	13.65			286.1
0.1	300 000	11.40			194.1
0.2	500 000	9.05	126.8	133.5	
0.5	400 000	8.30	89.5	101.6	99.5
0.75	400 000	8.05	52.0	62.5	
1.0	300 000	6.55	34.7	43.4	
2.0	300 000	5.25	18.5	22.8	
3.0	300 000	4.50	14.0	16.5	

[a] See text for definitions of σ_1, σ_2 and σ_{2-NOZP}.

2.2. Quasiclassical Trajectory Calculations. Our initial QCT calculations were done at relative translational energies (E_{trans}) greater than or equal to 0.2 kcal/mol; these are conventional QCT calculations, which are reviewed briefly below. To obtain the reaction cross section at each E_{trans} value, batches of 500 trajectories were integrated per impact parameter, b, ranging from 0 to b_{max} , where b_{max} (given in Table 1) is the maximum impact parameter for which exchange occurs. Typically reaction probabilities for fixed impact parameter, $P_R(b; E_{trans})$, were calculated every 0.25 Å except near b_{max} where they were calculated with a spacing of 0.05 Å. Cross sections were then obtained by numerically evaluating the integral

$$\sigma_R(E_{trans}) = \int_0^{b_{max}+0.05\ Å} 2\pi P_R(b; E_{trans})\, b\, db \quad (5)$$

For $E_{trans} = 1.0$ kcal/mol the calculations were extended to include 1000 trajectories at each impact parameter to estimate that the cross sections reported here are converged within 2−3%.

A modified version of the VENUS96 general chemical dynamics program[26] was used to sample reactant initial quasiclassical states, to integrate the classical equations of motion, and to analyze product state distributions. The initial HD internal coordinates and momenta associated with the "quasiclassical state" corresponding to the quantum ground rovibrational state (the only internal state significantly populated at the temperatures of interest here) were obtained by treating the diatomic as a rotating oscillator and determining the quantized energy of the "quasiclassical state" by Einstein−Brillouin−Keller (EBK)[27] semiclassical quantization of action. Values of the internuclear separation were randomly sampled according to the usual classical distribution. The initial momentum was determined from energy conservation and its sign randomly assigned. Separation of rotation and vibration was assumed in sampling quasiclassical initial conditions for the polyatomic ion CH_3^+. Rotational energy (and hence angular momentum) was chosen from a 10 K thermal distribution assuming CH_3^+ to be a symmetric top. A normal mode description was assumed for the CH_3^+ ground vibrational state. Normal mode amplitudes were assigned as $A_i = \sqrt{\hbar/\omega_i}$ where ω_i is the normal mode frequency. Normal mode phases were assigned randomly and the normal mode coordinates and velocities were determined from well-known results. The corresponding Cartesian coordinates and velocities were obtained by the standard linear transformation.[28] Quasiclassical vibrational and rotational quantum numbers were determined for the H_2 diatomic product. The rotational quantum number j was determined from the diatomic classical rotational angular momentum J by $J = \sqrt{j(j+1)}\hbar$. The vibrational quantum number was found by EBK quantization of vibrational action (assuming separability of rotation and vibration). The continuous quantities j and v were "binned" in

the standard manner to obtain quasiclassical product state distributions.[29]

The equations of motion were integrated with a sixth −order Adams-Moulton method using a time step of 0.05 fs. This step size was sufficient to ensure conservation of energy to six significant figures for the vast majority of trajectories (in excess of 98%) despite the occurrence of appreciable numbers of long-lived trajectories at all the energies considered here. Trajectories were initiated at an energy-dependent CH_3^+-HD separation distance that ranged up to 16 Å at the lowest value of E_{trans} considered here, 0.05 kcal/mol. The trajectories were then integrated until products had again separated to this distance or until an energy-dependent maximum number of integration steps had been exceeded (corresponding to 15.0−25.0 ps).

For the current choice of internal states of the reactants, i.e., ground vibrational states of HD and CH_3^+, ground rotational state of HD and a 10 K thermal distribution of rotational states of CH_3^+, the thermal rate constant was obtained from the reaction cross section using the standard expression:

$$k(T) = \left(\frac{8}{\pi\mu}\right)^{1/2} \frac{1}{(k_B T)^{3/2}} \int_0^\infty \sigma_R(E_{trans}) E_{trans} e^{-E_{trans}/k_B T} \, dE_{trans} \quad (6)$$

where k_B is the Boltzmann constant and μ is the reduced mass of the HD−CH_3^+ system.

For this ion−molecule reaction and the low temperatures of interest here the cross section must be known to quite low translational energies. This presents a number of computational challenges, not the least of which is the very long integration time needed to obtain complete trajectories. Our basic strategy is to fit $\sigma_R(E_{trans})$ to a general power law expression AE_{trans}^{-q} and to use this analytical expression in eq 6 to obtain $k(T)$.

As our work progressed, it became apparent that the standard QCT approach was becoming computationally prohibitive as E_{trans} decreased. The major source of this increase in effort is the number of trajectories that remain incomplete after a large number of integration steps. This is a consequence of the increasing lifetime of the collision complexes as E_{trans} decreases. Another source is the large increase in reaction cross section with decreasing E_{trans} (as discussed in more detail in section 3 below), which means that calculations have to be performed for a greater number of impact parameters. In addition as E_{trans} decreases and the reaction energy approaches the threshold region the concern about violation of "zero-point energy"[30] in the products increases.

To address the above issue of computational effort at our lowest relative translational energies (0.1 and 0.05 kcal/mol), and also to address the zero-point issue we adopted the following strategy. For these energies a different set of initial conditions was selected. The reactants were each set at their equilibrium geometries with zero vibrational energy, the rotational energy of CH_3^+ was sampled from a 10 K Boltzmann distribution and HD was given zero angular momentum as before and the relative orientations of the two reactants were randomly sampled. This approach designated as NOZP was used in a 1990 study of the O + H_2 system at collision energies up to 2 kcal/mol.[31] We also consider a simple hybrid approach where conventional QCT initial conditions are used but very long-lived trajectories are terminated before "completion" and a simple statistical treatment of these is used. Convergence of the results is then tested by extending the range of E_{trans} to lower values and using these various approaches to calculate the cross section.

3. Results and Discussion

3.1. Conventional QCT Calculations. Conventional QCT calculations (as described above) were performed at six E_{trans} values (shown in Table 1) between 0.2 and 3.0 kcal/mol. These calculations required over 2000 processor days on a Microway cluster equipped with Xeon 2.4 GHz processors. The calculations at E_{trans} = 0.2 kcal/mol alone required about 700 processor days. The convergence test at E_{trans} = 1.0 kcal/mol required approximately an additional 300 processor days. This time was basically caused by the large number of time steps required for the collision complex to dissociate.

Because the CH_4D^+ collision complex corresponds to a deep potential well, many trajectories become trapped near this region of the potential for prolonged periods of time. This is true of an increasing fraction of all trajectories as E_{trans} is reduced. We have chosen energy-dependent values of N_{max} , the maximum number of integration steps before a trajectory is terminated, that represent a compromise between minimizing computational cost and maximizing statistical validity. Values of N_{max} for the six collision energies at which cross sections were calculated from conventional QCT data are given in Table 1. These values resulted in more than 2/3 of all trajectories at each energy being followed to completion; for the four highest values of E_{trans} the fraction of trajectories that were followed to completion exceeded 3/4. In fact only two batches of trajectories (E_{trans} = 1.0 kcal/mol, b = 2.75 and 3.0 Å) resulted in completion rates less than 60% (59.0% and 57.2%, respectively). Given the large number of trajectories calculated (over 90 000) a detailed dynamical examination of each is infeasible. However, the observed trend in the probability of "long-time" collision events is consistent with increasing prevalence of collision complex formation with decreasing values of E_{trans}. For example, the fraction of trajectories with durations exceeding 5 ps increases monotonically from 34.8% at E_{trans} = 3.0 kcal/mol to 69.0% at E_{trans} = 0.2 kcal/mol. For comparison, at these two energies the typical durations of the shortest "direct" trajectories are about 0.3 and 1.0 ps, respectively. By "direct" we mean trajectories that either do not enter the region of the complex, or if they do, they do not remain in the complex region for more than several periods of oscillation.

The existence of "trapped" long-lived trajectories that cannot be integrated to completion with reasonable computational effort introduces some ambiguity into the calculation of $P_R(b; E_{trans})$ and the quantities that are ultimately determined from it, namely the cross section and the rate constant. Thus, we calculated $P_R(b; E_{trans})$ in two ways. In method 1, the contribution of "trapped" trajectories is ignored, and $P_R(b; E_{trans})$ is taken as the ratio of all reactive trajectories to all complete trajectories (those that have achieved asymptotic separation in N_{max} or fewer steps). At each collision energy, the outcomes of all trajectories at least 1 ps longer than the shortest "direct" trajectory at that energy were examined. This set of over 36 000 trajectories showed a 59.8% probability of isotope exchange. A survey of the outcomes of all completed trajectories with a duration of 2.5 ps or longer (over 32 000 trajectories) shows that 62.9% of these trajectories result in isotope exchange. Both these results (over all energies considered) are reasonably close to the 60% exchange yield that would be exhibited by a CH_4D^+ complex that "forgets" the details of its formation and behaves statistically with regard to the H/D composition of the diatomic product. It therefore seems a reasonable approximation to assume that all "trapped" trajectories will behave statistically. Thus, in our method 2, for a given b and E_{trans}, if the number of completed reactive trajectories is N_R and the number of "trapped" (not

having achieved the asymptotic separation threshold after N_{max} steps) trajectories is N_T

$$P_R(b; E_{trans}) \equiv \frac{N_R(b; E_{trans}) + 0.6N_T(b; E_{trans})}{N_{total}(b; E_{trans})} \qquad (7)$$

where $N_{total}(b; E_{trans})$ is the total number of trajectories run at an impact parameter b and collision energy E_{trans}.

It is also worth noting that the reaction probability $P_R(b; E_{trans})$ for completed trajectories is found to be a nearly constant function of b for $b < b_{max}$ and then decreases quickly to zero over a range of roughly 1 bohr at the lowest value of E_{trans}, 0.2 kcal/mol. At the highest E_{trans} we considered, 3 kcal/mol, the decrease occurs more gradually over a range of roughly 2 bohr.

Table 1 gives the reaction cross sections, denoted $\sigma_1(E_{trans})$ and $\sigma_2(E_{trans})$, calculated using methods 1 and 2, respectively, for the determination of P_R (b; E_{trans}). In both cases the cross sections fall off monotonically with increasing values of E_{trans} as would be expected for an ion−molecule reaction such as this one. Note $\sigma_2(E_{trans}) > \sigma_1(E_{trans})$ for all values of E_{trans} in Table 1. This is easily understood. By excluding the "trapped" trajectories, method 1 gives increased weight to "direct" trajectories, only a small fraction (substantially less than 0.6) of which lead to isotope exchange, compared to incomplete "complex" trajectories which are included in method 2 and which are assumed to lead to reaction products with probability 0.6. As we have seen the latter appear to achieve a statistical (or perhaps slightly higher) level of exchange. In contrast the exchange probability for "direct" trajectories varies from a few percent to several percent for the values of E_{trans} examined here.

We examined the internal state distributions of the products obtained by the conventional QCT method. Of course the internal energies are continuous and standard histogram binning was done to assign quantum states. Consider the H_2 product first. As one might anticipate for the low collision energies considered here, essentially all of the H_2 products emerge in the $v = 0$ vibrational state. A small fraction (less than 0.4% at all E_{trans} values shown in Table 1) of products are "binned" into $v = 1$, though their classical vibrational actions are closer to h than to $3h/2$.

A great many H_2 products that are "binned" into the $v = 0$ state have classical actions less than $h/2$, that is, their asymptotic vibrational energy is less than the quantum zero-point energy (ZPE). These trajectories we refer to as "ZPE noncompliant" and they can have important consequences since the "excess" energy can appear in other degrees of freedom, e.g., the H_2 rotational state distribution. To illustrate this we plot this distribution in Figure 1 as rotational state specific cross sections for four selected values of E_{trans}. As seen there, a modest amount of rotational excitation of the H_2 product occurs with all four rotational distributions peaking at j values of 2 or 3. However, the tails of the distributions extend out as far as $j = 10$. Quantum mechanically the maximum amount of energy available for product excitation should be $E_{trans} + \Delta H$ where ΔH is the reaction exothermicity (309 cm^{-1} on the JBB surface). Thus, even at the largest value of E_{trans} (3.0 kcal/mol, approximately 1050 cm^{-1}) for H_2 with a rotational constant of approximately 61 cm^{-1}, the maximum allowed rotational quantum number should be $j = 4$. However, at this energy the fraction of the exchange cross section associated with quantum mechanically inaccessible ($j > 4$) rotational states is nearly 25%. For the lowest two E_{trans} values (0.5 and 0.2 kcal/mol), this fraction exceeds 50%. Since the total energy is a constant, the rotational energy associated with these quantum mechanically inaccessible rotational states must come at the expense of the vibrational zero-point energies of the H_2 and CH_2D^+ products.

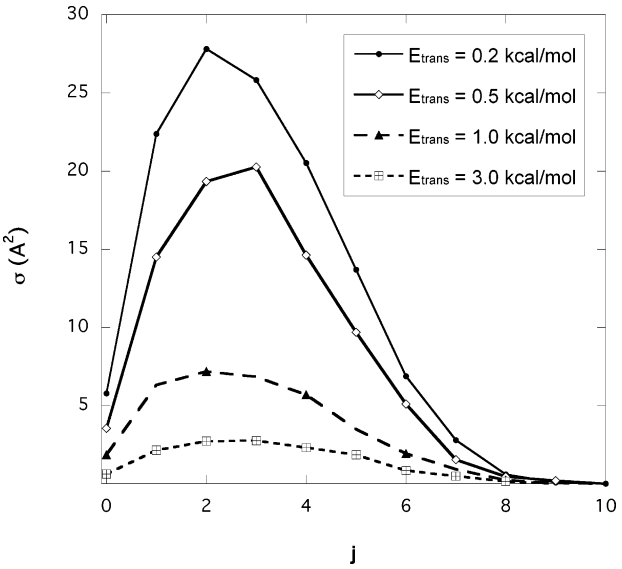

Figure 1. Cross sections to form product H_2 in indicated rotational state, j, vs j at selected collision energies from conventional QCT calculations.

The vibrational energy distribution of the CH_2D^+ product is shown in Figure 2 for two initial translational energies. As seen the distributions are nearly Gaussian with an average (and most probable) value of roughly 18 kcal/mol, which is actually quite close to the zero-point energy of CH_2D^+. We made no attempt to bin the vibrational energies; however, as seen, most trajectories lead to CH_2D^+ that would be assigned to the ground vibrational state; however, as with H_2 there are substantial numbers of trajectories that emerge with less than zero-point energy in the CH_2D^+ product.

Since the focus of this paper is not the vibration/rotation distributions of the reaction products we are not overly concerned about the effects of "ZPE noncompliance" on these distributions. However, we are concerned about this at the level of the thermal rate constant and for that reason we also performed calculations without ZPE. The results of these calculations are described next.

3.2. NOZP Trajectory Calculations. On the basis of the above discussion of "ZPE noncompliance" we performed trajectory calculations without giving the reactants zero-point energy. This also has the benefit of reducing the computational effort, which is considerable, as already noted. For E_{trans} below 0.2 kcal/mol we estimated $O(10^3)$ processor days per collision energy using conventional QCT. Therefore, we used the NOZP trajectory approach described in section 2 above to obtain cross sections below $E_{trans} = 0.2$ kcal/mol.

To test the reliability of this approach we first performed calculations at $E_{trans} = 0.5$ kcal/mol, an energy at which $\sigma_2(E_{trans})$ had already been determined from conventional QCT calculations. Initially 250 trajectories that randomly sampled the orientation between the reactant fragments were performed at each impact parameter. Examination of these trajectories showed them (and all of our other NOZP trajectories) to fall into two distinct classes: "direct" trajectories that can be integrated to completion and do not produce any isotope exchange, and "trapped" trajectories that cannot be integrated to completion in 400 000 integration steps. Thus, the reaction probability at each impact parameter was determined from eq 7 with $N_R = 0$ and a cross section denoted σ_{2-NOZP} given in

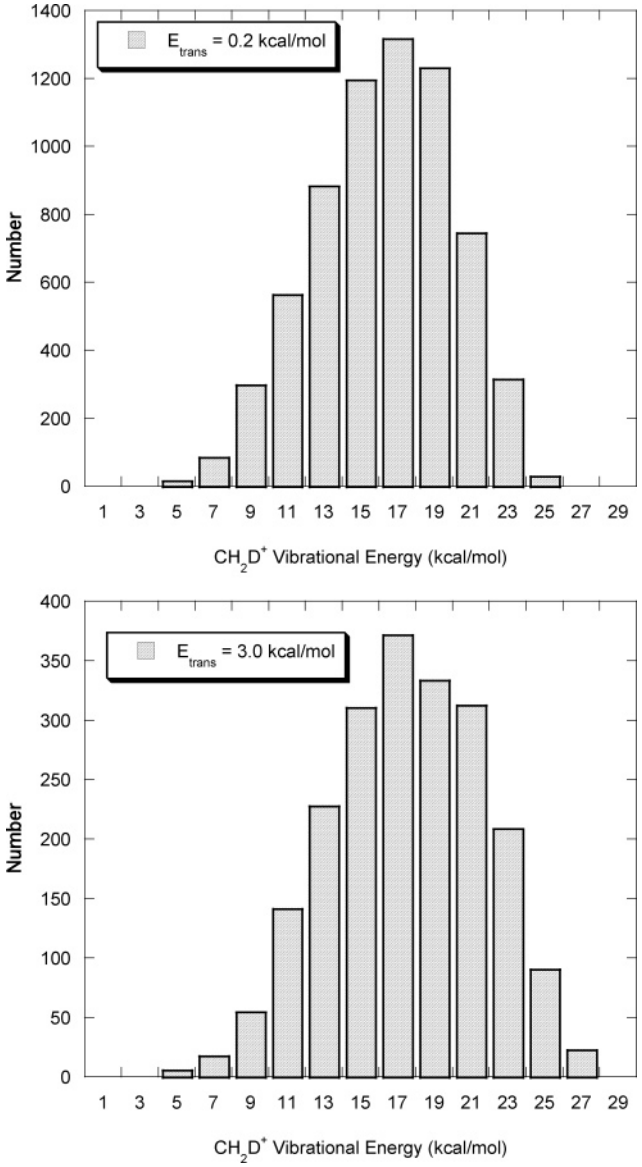

Figure 2. Internal energy distributions of product CH_2D^+ for the initial translational energies indicated.

Table 1 was calculated using these probabilities. Clearly at this energy there is excellent agreement between σ_2 and $\sigma_{2-\mathrm{NOZP}}$, with the two results differing by only about 2%. Convergence with respect to the number of NOZP trajectories was examined by repeating this calculation using only 100 trajectories per impact parameter. This resulted in a value of $\sigma_{2-\mathrm{NOZP}} = 100.3$ Å,[2] which differs from the result given in Table 1 (based on 250 trajectories per impact parameter) by less than 1%. Thus, to limit the computational cost of our calculations at collision energies of 0.05 and 0.1 kcal/mol, we have used 100 trajectories per impact parameter for computing $P_R(b; E_{\mathrm{trans}})$ and the resultant cross sections. These $\sigma_{2-\mathrm{NOZP}}$ cross sections at these two lowest collision energies are given in Table 1.

It is interesting and obvious that fewer trajectories are needed in NOZP calculations since the phase space associated with the vibrational degrees of freedom is not sampled. However, the trajectories are extremely long-lived and as a result we had to resort to a statistical approximation to obtain the reaction probability. This approximation was tested and justified using conventional and much more CPU intensive QCT calculations. In the absence of these tests, the validity of the statistical approximation would be unknown, of course.

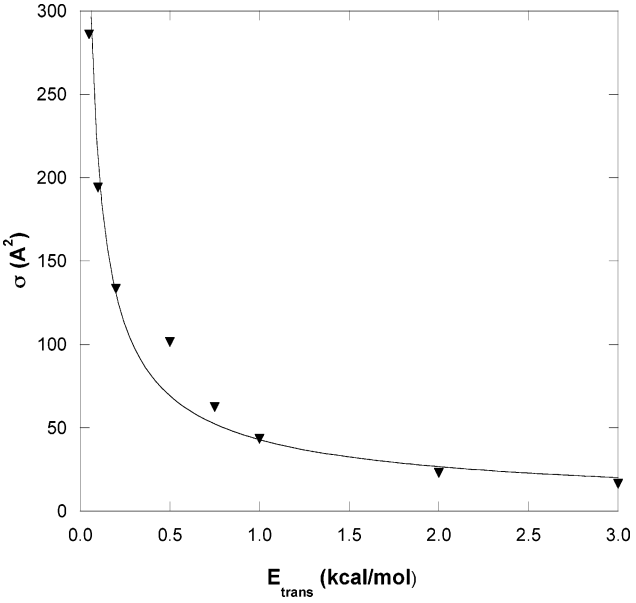

Figure 3. Energy dependence of $\sigma_{2-\mathrm{extended}}$ vs E_{trans}. See text for the definition of $\sigma_{2-\mathrm{extended}}$.

TABLE 2: Fitting Parameters for the Energy (Joules) Dependence of the Cross Sections (m^2)

data set	A	q	R
σ_2–extended	5.4297×10^{-33}	0.68944	0.98708
σ_2	9.4367×10^{-36}	0.82684	0.94687
σ_1	8.4342×10^{-37}	0.87528	0.95934

3.3. Rate Constant Calculations. We cannot compute reaction cross sections down to the lower limit, $E_{\mathrm{trans}} = 0$ of the integral expression for the thermal rate constant given by eq 6 and so an extrapolation to that limit is necessary. The NOZP approach has allowed the present calculations to go as low as $E_{\mathrm{trans}} = 0.05$ kcal/mol. Substantial computational effort would be required to add even a single additional data point in the range $E_{\mathrm{trans}} = 0.01-0.02$ kcal/mol (even using the NOZP approach) and so we have extrapolated our results down to E_{trans} using the cross sections down to $E_{\mathrm{trans}} = 0.05$ kcal/mol. We did this by fitting the energy dependence of the cross sections to the form AE_{trans}^{-q}. Figure 3 shows our most extensive data set, denoted $\sigma_{2-\mathrm{extended}}$ consisting of the union of the σ_2 ($E_{\mathrm{trans}} = 0.2-3.0$ kcal/mol) and $\sigma_{2-\mathrm{NOZP}}$ ($E_{\mathrm{trans}} = 0.05-0.10$ kcal/mol) data, as well as the least-squares optimized power law fit to this data set. Obviously the fit is less than perfect but it is very good in the low-energy regime that contributes most to the rate constant at 10 K. We performed similar fits for the σ_1 and σ_2 data sets obtained from conventional QCT calculations; however, these fits were restricted to data at translational energies greater than or equal to 0.2 kcal/mol. The parameters for the three fits (using energy in joules and cross section in square meters) are given in Table 2. As seen the fitting parameters for σ_1 and σ_2 are close to each other, but differ significantly from the fitting parameters for $\sigma_{2-\mathrm{extended}}$. This shows the sensitivity of the fit to the inclusion of low-energy data and indicates that the fit to $\sigma_{2-\mathrm{extended}}$ is the preferred one. To determine whether the data used to fit $\sigma_{2-\mathrm{extended}}$ is sufficient to obtain a "converged" set of parameters we redid the fit to $\sigma_{2-\mathrm{extended}}$ excluding the lowest energy cross section at 0.05 kcal/mol. The resulting parameters, $A = 5.5188 \times 10^{-33}$ and $q = 0.73836$ (in the units used in Table 2), differ by 5 and 7% from the respective parameters determined using all the data. This level of difference gives us some confidence that the parameters for the fit to

TABLE 3: Thermal Rate Constants (10^{-9} cm^3/s) for $CH_3^+ + HD \rightarrow CH_2D^+ + H_2$ at 10 K

$k_{2-\text{extended}}$	1.67 ± 0.4
k_1	3.14
k_2	3.01
k_{expt} (ref 12)	1.65 ± 0.10
k_L[a]	0.80

[a] The Langevin rate constant to form the complex multiplied by a statistical factor of 0.6.

$\sigma_{2-\text{extended}}$ in Table 2 are fairly well converged. Below we will examine the differences in the rate constant obtained from these fits.

The various fits were each used in eq 6 to generate three different approximations to the thermal rate constant at 10 K, denoted $k_{2-\text{extended}}$, k_1 and k_2, respectively. For the chosen power law expression for the energy dependence of the cross section, AE_{trans}^{-q}, the integral in eq 6 can be done analytically to obtain the following expression for the thermal rate constant:

$$k(T) = \left(\frac{8}{\pi\mu}\right)^{1/2} (kT)^{1/2-q} A\Gamma(2-q) \tag{8}$$

where $\Gamma(x)$ is the standard gamma function which was evaluated numerically.[32] Table 3 gives our values of the thermal rate constant for the exchange reaction at 10 K along with the experimental value k_{expt} of Asvany et al.[12] Also included there is the Langevin approximation to the rate constant for an ion−molecule reaction which here we base on the well-known expression for the rate constant to form the complex

$$k_L = 2\pi e(\alpha/\mu)^{1/2} \tag{9}$$

where μ and α are the reduced mass in grams and the electric dipole polarizability in cm^3, respectively of the nonpolar reagent, HD,[33] and e is the electron charge in electrostatic units. In the present case we have modified k_L of eq 9 by multiplying it by the statistical factor, 0.6, which describes the statistical breakup of the complex to form the products, as discussed above. As can be seen in Table 3, $k_{2-\text{extended}}$ is in excellent (though perhaps fortuitous) agreement with the experimental value. The k_1 and k_2 values are both substantially larger (by almost a factor of 2) than the experimental value which clearly indicates that extrapolation of the energy dependence of the cross sections below the lower limit of those data sets, $E_{\text{trans}} = 0.2$ kcal/mol, causes significant error in the rate constant calculation at 10 K and underscores the importance of having as much low-energy data as possible to minimize the extent of the extrapolation. To test the sensitivity of $k_{2-\text{extended}}$ to the extrapolation in $\sigma_{2-\text{extended}}$ we used the fit to the $\sigma_{2-\text{extended}}$ data set excluding the $E_{\text{trans}} = 0.05$ kcal/mol data point described above and redid the rate constant calculation and obtained a value of 2.04×10^{-9} cm^3/s. This result suggests that a conservative uncertainty estimate for our $k_{2-\text{extended}}$ value is about 4×10^{-10} cm^3/s. The simple Langevin approach underestimates the experimental value by approximately a factor of 2.

The Langevin rate constant given by eq 9 (which is based on a model in which the cross section varies like $E_{\text{trans}}^{-1/2}$) is temperature independent as is well-known and as can be seen from eq 8. The rate constant obtained using the fit corresponding to the $\sigma_{2-\text{extended}}(E_{\text{trans}})$ data has a predicted weak inverse temperature dependence, $T^{-.18944}$. If we assume that an increase in the rotational temperature from 5 to 50 K has only negligible effect on the reaction cross section, then we can use our results to estimate the thermal rate constant in this temperature regime. Figure 4 shows a plot of our results for the thermal rate constant

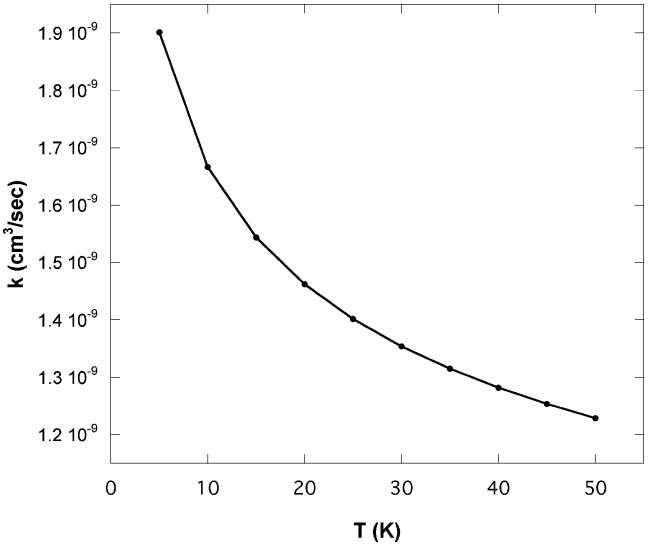

Figure 4. Temperature dependence of the thermal rate constant $k_{2-\text{extended}}$ for $CH_3^+ + HD \rightarrow CH_2D^+ + H_2$ between 5 and 50 K.

in the 5−50 K temperature range. The rate constant can be seen to decline only by about 35% within this temperature range. This weak, inverse T dependence is certainly consistent with the usual behavior of the rate constants of ion−molecule reactions at the temperature of the ISM.

4. Summary and Conclusions

A new full-dimensional ab initio PES with the correct asymptotic electrostatic interactions for the CH_5^+ system has been used with quasiclassical trajectory methods to determine cross sections for reaction 1 at low relative translational energies, E_{trans}, in order to obtain the low-temperature thermal rate constant, which is of interest in astrochemistry. The conventional quasiclassical trajectory approach becomes prohibitive at the low energies necessary to obtain the cross section for the calculation of the rate constant. Thus, trajectory calculations with no zero-point energy of the reactants were done at very low energies. These "no zero-point energy" calculations were validated by comparing the cross section obtained with them to that obtained using the conventional approach at one translational energy. A combination of the conventional method along with some calculations employing no zero-point energy of the reactants was done in order to obtain the cross section to relative translational energies as low as 0.05 kcal/mol. A power law fit to the energy dependence of this data has been used to extrapolate to $E_{\text{trans}} = 0$ so that the thermal rate constant at 10 K for the exchange process could be obtained. Our best calculated rate constant is 1.67×10^{-9} cm^3/s, with estimated uncertainty of 25%, which is in very good agreement with the experimental value of Asvany et al.[12] The calculated rate constant has a slight negative temperature dependence which was explicitly shown for T between 5 and 50 K.

Finally we note that it would be of interest to apply sophisticated statistical approaches to this reaction, such as the "Statistical Adiabatic Channel Model",[34] and we hope to do that in the future.

Acknowledgment. K.M.C. thanks Augustana College for sabbatical leave support for the period during which this work was performed, and Prof. Aaron Dinner and his research group for their hospitality at the University of Chicago where the first draft of this paper was written. J.M.B. thanks the National Science Foundation (CHE-0446527) for financial support.

References and Notes

(1) Herbst, E. *Space Sci. Rev.* **2002**, *95/96*, 1.
(2) Smith, D. *Chem. Rev.* **1992**, *92*, 1473.
(3) Gerlich, D.; Herbst, E.; Roueff, E. *Planet. Space Sci.* **2002**, *50*, 1275.
(4) Asvany, O.; Schlemmer, S.; Gerlich, D. *Astrophys. J.* **2004**, *617*, 685.
(5) Gerlich, D. *Phys. Chem. Chem. Phys.* **2005**, *7*, 1583.
(6) Tal'roze, V. L.; Lyubimova, A. K. *Dokl. Akad. Nauk. SSSR* **1952**, *86*, 909.
(7) Schreiner, P. R. *Angew. Chem., Int. Ed.* **2000**, *39*, 3239.
(8) Marx, D.; Parrinello, M. *Nature (London)* **1995**, *375*, 216.
(9) Marx, D.; Parrinello, M. *Science* **1996**, *271*, 179.
(10) Marx, D.; Parrinello, M. *Z. Phys. D* **1997**, *41*, 253.
(11) White, E. T.; Tang, J.; Oka, T. *Science* **1999**, *284*, 135.
(12) Asvany, O.; Kumar, P. P.; Redlich, B.; Hegemann, I.; Schlemmer, S.; Marx, D. *Science* **2005**, *309*, 1219.
(13) Kumar, P. P.; Marx, D. *Phys. Chem. Chem. Phys.* **2006**, *8*, 573.
(14) Huang, X.; McCoy, A. B.; Bowman, J. M.; Johnson, L. M.; Savage, C.; Dong, F.; Nesbitt, D. J. *Science* **2006**, 311, 60.
(15) Brown, A.; Braams, B. J.; Christoffel, K.; Jin, Z.; Bowman, J. M. *J. Chem. Phys.* **2003**, *119*, 8790.
(16) McCoy, A. B.; Braams, B. J.; Brown, A.; Huang, X.; Jin, Z.; Bowman, J. M. *J. Phys. Chem. A* **2004**, *108*, 4991.
(17) Brown, A.; McCoy, A. B.; Braams, B. J.; Jin, Z.; Bowman, J. M. *J. Chem. Phys.* **2004**, *121*, 4105.
(18) Jin, Z.; Braams, B. J.; Bowman, J. M. *J. Phys. Chem. A* **2006**, *110*, 1569.
(19) Hampel, C.; Peterson, K.; Werner, H.-J. *Chem. Phys. Lett.* **1992**, *190*, 1.
(20) Dunning, T. H. *J. Chem. Phys.* **1989**, *90*, 1007.
(21) Xie, Z.; Braams, B. J.; Bowman, J. M. *J. Chem. Phys.* **2005**, *122*, 2226.
(22) Bowman, J. M.; Gazdy, B.; Schafer, P.; Heaven, M. C. *J. Phys. Chem.* **1990**, *94*, 2226.
(23) Prosmiti, R.; Buchachenko, A. A.; Villarreal, P.; Delgado-Barrio, G. *Theor. Chem. Acc.* **2001**, *106*, 426.
(24) Kolos, W.; Wolniewicz, L. *J. Chem. Phys.* **1967**, *46*, 1426.
(25) Wolniewicz, L.; Simbotin, I.; Dalgarno, A. *Astrophys. J. Suppl. Series* **1998**, *115*, 293.
(26) Hase, W. L.; Duchovic, R. J.; Hu, X.; Kominicki, A.; Lim, K. F., Lu, D.-H.; Peslherbe, G. S.; Swamy, K. N.; Vande Linde, S. R.; Varandas, A.; Wang, H.; Wolf, R. J. *QCPE Bull.* **1996**, *16*, 43.
(27) Gutzwiller, M. C. *Chaos in Classical and Quantum Mechanics;* Springer-Verlag: New York, New York, 1990.
(28) Wilson, E. B.; Decius, J. C.; Cross, P. C. *Molecular Vibrations*; Dover Publications: New York, 1980.
(29) Sewell, T. D.; Thompson, D. L. *Int. J. Modern Phys. B* **1997**, *11*, 1067.
(30) Xie, Z.; Bowman, J. M. *J. Phys. Chem. A* **2006**, *110*, 5446.
(31) Nyman, G.; Davidsson, J. *J. Chem. Phys.* **1990**, *92*, 2415.
(32) Press, W.H.; Teukolsky, S.A.; Vetterling, W.T.; Flannery, B.P. *Numerical Recipes in Fortran,* 2nd ed.; Cambridge University Press: New York, 1992.
(33) Olney, T. N.; Cann, N. M.; Cooper, G.; Brion, C. E. *Chem. Phys.* **1979**, *223*, 59.
(34) Troe, J. *J. Chem. Phys.* **1983**, *79*, 6017.